Paper No. 1649. (quote when citing this article)
Eleventh World Conference on Earthquake Engineering
ISBN: 0 08 042822 3

SITE AMPLIFICATION OF GROUND MOTIONS DURING THE 1995 HYOGO-KEN NANBU EARTHQUAKE, JAPAN, IN SEVERELY DAMAGED ZONE

TOMOTAKA IWATA, KEN HATAYAMA, and ARBEN PITARKA

Disaster Prevention Research Institute, Kyoto University.
Gokasho, Uji, Kyoto, 611, Japan
[TEL/FAX 0774-33-5866 e-mail: iwata@egmdpri01.dpri.kyoto-u.ac.jp]

ABSTRACT

Site amplifications during aftershocks of the 1995 Hyogo-ken Nanbu earthquake were examined in and around disaster area of Higashinada Ward, Kobe city, Japan. Five temporary stations together with the KOB station (CEORKA) for strong ground motion observations were installed just after the mainshock to arrange an array just across the severe damage band of about 1.5km wide. Several aftershock records were obtained among these stations. The peak values of the observed ground accelerations and velocities at the soil sites were 3 to 20 times larger than those at the rock site. Spectral ratios between the soil sites and the rock site have peak frequencies characteristic to each station pair. We also estimated a thickness of about 1km for the sedimentary basin just under the soil sites using SP-converted waves appeared at all soil sites. Waveform simulations using a dislocation point source in two-dimensional underground structure model were performed to explain the observed records both at the rock and the soil stations. We found that large amplifications at the soil sites are generated by not only basin-edge effect but the low-velocity surface layers. The heavy damage caused by the mainshock is therefore strongly connected with the sedimentary structure.

KEYWORDS

The 1995 Hyogo-ken Nanbu (Kobe) earthquake, site amplification, basin structure, aftershock observation, basin-edge effect, Finite Difference Method

1. INTRODUCTION

On January 17, 1995, the 1995 Hyogo-ken Nanbu earthquake struck the Kobe City and the Awaji Island, Hyogo Prefecture in the Kansai area of Japan. Large disasters such as highway collapse, building and house failures, and widespread fires occurred mainly in the downtown areas of Kobe. An isoseismal map (Japan Meteorological Agency, 1995) shows that a belt zone of heavy disaster of Japanese seismic intensity 7 runs east-northeast to west-southwest across the city.

A similar concentrated earthquake disasters occurred in the Sherman Oaks and the Santa Monica regions during the 1994 Northridge earthquake, California, U.S.A. Graves(1995) tried to simulate the large amplitude and long period later phases appearing in the strong ground motion records during the mainshock observed at the Santa Monica City Hall using two dimensional basin structure modeling. He concluded that a combination of both large-scale (deep basin) and small-scale (shallow micro-basin) structures are needed to explain the observed site responses. Gao et al.(1995) found a localized large site amplification in the disaster area from array observation of aftershocks. They interpreted the localized amplification as a focusing effect by the edge of the sediments.

In this study, to investigate the cause of spatial disaster distribution, we made an array observation of aftershocks in downtown Kobe. The purposes are (1) to compare site effects between severely damaged and slightly damaged or no-damaged areas, and (2) to study the effects of surface geology on seismic motions. Some results of the observation have already reported by Iwata et al.(1995a) and Iwata et al.(1995b), and waveform simulations are performed by Pitarka et al.(1995).

2. ARRAY OBSERVATION

From January 18, 1995, the cooperative strong motion observation group started to deploy strong motion observation stations in the source region. Finally, up to the beginning of February, the group installed more

than 30 observation stations (The cooperative strong motion observation group, 1995). This temporary observation has continued to the end of March, 1995. We installed the stations in Higashinada Ward; the easternmost part of the Kobe City, where severely damaged wooden houses were concentrated in a narrow band about 1.5km wide. Totally, five temporal observation stations were installed close to the permanent station (KOB) of the Committee on Earthquake Observation and Research in the Kansai Area (CEORKA) (Toki et al., 1995). In Fig. 1, we show the location map of the stations used in this study together with the seismic intensity map (JMA, 1995). Largest aperture of this array is about 3km. According to the geological map (Hujita and Kazama, 1982), the KMC station is a rock site, whereas KOB, FKI, NOM, and ASY stations are installed on alluvium, and the FKE station on a sand bank (Table 1). The FKI, NOM, and ASY stations are located in the severely damaged band and the KOB and FKE stations are in the vicinity.

All seismometers were fixed either on the free surface or in the basement of one-story buildings. The observation system consists of velocity or acceleration seismometers with a wide-frequency-band (0.02 to 30Hz), a high-dynamic-range (>80db, up to 20cm/s or 1g), and an event-trigger recorder with pre-trigger memory. Recording media are either IC-card or MO-disk. Each station has an own clock calibrated by radio time signals. From January 19 to February 18, more than eighty records are observed at six stations including the KOB station. We analyzed nine aftershock records obtained at almost all stations.

3. DATA ANALYSIS

We show the epicenter distribution of the aftershocks in Fig. 2 and the hypocenter parameters determined by JMA in Table 2. In Fig. 3, we show examples of observed ground accelerations at the five stations during the event of 23:16, January 25 and those at the six stations during the event of 16:19, February 2. Data were recorded by either the velocity seismometers or accelerometers. Data by the velocity seismometers are differentiated to accelerations in the frequency domain. Those acceleration data were low-pass-filtered with a cut-off frequency of 15Hz.

The horizontal peak values of the ground acceleration at the soil sites are 3 to 20 times larger than those at the rock site (KMC) as shown in Fig. 3. In particular, there are very large peak accelerations at the FKI, ASY, NOM, and FKE stations. There also are a distinct phase as well especially in the vertical component between the P and S arrivals at all the soil site stations. This phase appears on all records analyzed. This is a SP phase converted at the interface between the sediment and basement rock because it is not seen at the rock site. We will estimate the thickness of sediments using this phase in Section 4-1.

The spectral amplitude ratios of the soil sites to the rock site, KMC, are given in Fig. 4. We made no correction of geometrical spreading for calculation of the spectral ratio. The time window length is 10.24s, including the S-wave part, and spectral amplitude ratios in the frequency range between 1 and 10Hz are shown in the figure. The ratios are calculated from the smoothed spectra of the vectorial summation of the 10% running mean of the two horizontal components. Large amplitude ratio of 3 to 20 times are obtained over this frequency range. Spectral ratios scatter widely among events and this might be affected by the source radiation effects of events and the complex underground structure in this array area. However, each spectral ratio of the specific station pair has an average tendency. The predominant frequencies of the ratios vary with the sites; 5Hz for KOB/KMC, 3-5Hz for NOM/KMC, 2Hz for FKI/KMC, 2-4Hz for ASY/KMC, and 2Hz for FKE/KMC. The variation of predominant frequencies reflect the thickness variation of surface soft deposits beneath the soil sites, and the large amplifications around 2-4Hz at the FKI, ASY, and FKE stations are strongly connected with the heavy damage there.

4. DISCUSSION

4-1 Estimation of thickness of sediment using the SP-converted wave

Here, we will estimate the thickness of sediments beneath the soil stations using SP-converted waves. We read the time difference between S and SP phases on each record by eyes and show the time difference at each station in Fig. 5. The S-SP time differences take characteristic values at each station. Referring the P- and S-wave velocity values are given for the sediments of the Osaka basin modeled by Kagawa et al. (1993), we assume the S-wave velocity of 0.65km/s and the P-wave velocity of 2.5km/s for the sediment layer and 3.2km/s and 5.7km/s for the bedrock. We calculated the theoretical S-SP time of one-dimensional velocity structure model using the given hypocenter for each station-event pair. For each station, we estimated the thickness of sediments so that the sum of residual time between the observed S-SP times and the theoretical ones has a minimum value.

Fig. 6 shows the estimated thickness of sediment under each observation station. Thicknesses of sediments are 0.7-1.1km. Even under the KOB station, which is the closest observation site from the edge of the basin (horizontal distance is less than 1km), the thickness of sediment is about 0.8km. These

assumptions such as the uniform velocity structure and the vertical incidence are oversimplified. However, quite important result is that the slope of the edge of basin is seems to be almost vertical from the existence of SP converted wave of the records at the KOB station. A reflection survey using an artificial source was done near our array site to determine edge shape of sediments after the mainshock (CEORKA, 1995, personal communication). In that cross section, there exist several thrusting-type faults around the edge of the basin and the thickness of sediments was supposed to more than 1km. Our estimation of thickness of sediments using the SP converted wave coincides with the result of reflection survey.

4-2 Modeling of underground structure through waveform simulations

In order to explain the ground motion amplifications of aftershocks, we performed two-dimensional numerical simulation of the ground motions at the stations KMC, KOB, FKI and FKE. The ASY and NOM stations are slightly apart from a line passing through the epicenter and other stations. The simulation is aimed at reproducing the waveforms of the transverse component of the observed motion. The simplified basin geometry used in this simulation is based on a reflection survey profile passing close to the site (CEORKA, personal communication). The total thickness of the sediment is assumed from the previous result of 4-1. The velocity structure and the attenuation is proposed by Iwata et al.(1995a, b). In our simulation, we considered a layered profile as shown in Fig. 7.

Finite-difference schemes are used to simulate the propagation of seismic waves in the heterogeneous model. We introduce an intrinsic attenuation for the structure and a radiation pattern of the point dislocation source. Upper frequency limit of accurate calculation is set to be 3Hz. Source radiation information is from Katao(1995) and Iwata et al.(1995). The seismic moment was scaled by fitting overall amplitude Fourier spectra of the transverse component of the ground motion recorded at the KMC station at frequencies less than 2Hz.

In Fig. 8, we show the synthetic and the observed velocity during the January 25 event. The synthetics and the data are filtered with a band-pass-filter of 0.1-3Hz. From this comparison, qualitative agreement between the simulated and the observed ground motions at the sediment site. The simulation show very large amplification due to the local structure at the FKI station and a relatively lower one at the FKE station. This is caused by the constructive superposition between the diffracted wave generated by the basin-edge and the direct wave near the FKI station. However, quantitatively, the simulation is poor than the observed records at the sediment sites. The thin shallow layers, not included in this two-dimensional velocity model simulation, may amplify the ground motion at frequencies higher than 1Hz. Their inclusion requires finite-difference calculations in a very fine grid. Pitarka et al.(1995) recovered the amplitudes of simulations by adding the thin surface layer with one-dimensional transfer function technique.

5. CONCLUSIONS

Array aftershock observations were made in Higashinada Ward, Kobe City, to estimate the site responses in severely and slightly damaged areas. Five temporary stations for strong ground motion observations were installed just after the mainshock to arrange an array across the severe damage band of about 1.5km wide. From the several aftershock data, we found that the peak values of the observed ground accelerations and velocities during aftershocks at the soil sites were 3 to 20 times larger than those at the rock site. The spectral ratio for the soil site in the damaged area to the rock site is larger than 10 in the frequency range of 2 to 4Hz.

Using SP-converted waves appeared at all soil sites, we estimated thickness of the sedimentary basin just under the soil sites. Thickness of sediments were estimated about 0.7km to 1.1km under the soil sites. Waveform simulations using a dislocation point source in two-dimensional underground structure model were performed to explain the observed records both at the rock and the soil stations. We found that large amplifications at the soil sites are generated by not only basin-edge effect but the low-velocity surface layers. The heavy damage caused by the mainshock is therefore strongly connected with the sedimentary structure.

Acknowledgments

We are grateful to CEORKA and its secretary, Takao Kagawa for assistance given. Discussions with Kojiro Irikura and Hiroshi Kawase are useful. We also thank Koji Matsunami, Haruko Sekiguchi, Shin'ichi Matsushima, and Toshimi Satoh for their help to deploy and/or maintain instruments. KMC (Kobe Medical College), FKI (Fukuike elementary school), ASY (Seido elementary school) , NOM (Motoyama daini elementary school), and FKE (Kobe Merchant Marine College) kindly allowed us to install our instruments, though many refuges are still there.

REFERENCES

The cooperative strong motion observation group (1995). Cooperative strong motion observations in the fault area of the 1995 Hyogoken-nambu earthquake, *Reports on the 1995 Hyogoken-nambu earthquake and its disaster, granted from the Japanese Ministry of Education, Science and Culture (No. 06306022)*, 124-154.

Gao, S., H. Liu, P. M. Davis, and L. Knopoff, Localized amplification of seismic waves and correlation with damage due to the Northridge earthquake, *submitted to Bull. Seism. Soc. Am.*, 1995.

Graves, R. W. (1995). Preliminary analysis of long-period basin response in the Los Angeles region from the 1994 Northridge earthquake, *Geophys. Res. Let.*, **20**, 101-104.

Hujita, K. and T. Kazama (1982). Geology of the Osaka-Seihokubu District. Quadrange Series, Scale 1:50,000, Geol. Surv. Japan, 112p. (in Japanese with English Abstract)

Iwata, T., K. Hatayama, H. Kawase, K. Irikura, and K. Matsunami (1995a). Array observation of aftershocks of the 1995 Hyogoken-nambu earthquake at Higashinada ward, Kobe city, *J. Natural Disas. Sci.*, **16**, 41-48.

Iwata, T., K. Hatayama, H. Kawase, and K. Irikura (1995b). Site amplification of ground motions during aftershocks of the 1995 Hyogo-ken Nanbu earthquake in severely damaged zone - Array observation of ground motions at Higashinada Ward, Kobe city, Japan -, *submitted to J. Phys. Earth.*

Japan Meteorological Agency (1995). Seismic intensity VII area. *Report of the Coordinating Committee for Earthquake Prediction, the 113 meeting,* (in Japanese).

Kagawa, T., S. Sawada, Y. Iwasaki, and J. Nanso (1993). Modeling of the deep underground structure of the Osaka basin, *Proc. 22th JSCE Earthq. Eng. Symp.*, 199-202.

Katao, H. (1995). Source mechanisms of aftershocks of the 1995 Hyogoken-nambu earthquake, *Report of the Coordinating Committee for Earthquake Prediction, the 115 meeting,* (in Japanese).

Pitarka, A., K. Irikura, T. Iwata, and K. Kagawa, (1995). Was the basin edge geometry responsible for the damage concentration in Higashinada-ku during the 1995 Hyogoken-nanbu (Kobe) earthquake?, *submitted to J. Phys. Earth.*

Toki, K., K. Irikura, and T. Kagawa(1995). Strong motion records in the source area of the Hyogoken-nambu earthquake, January 17, 1995 Japan, *J. Natural Disas. Sci.*, **16**, 23-30.

Table 1 List of array observation stations in Higashinada Ward, Kobe City. The geological condition at each station is based on the geological map of Hujita and Kazama (1982).

CODE geological condition	LAT. (N) deg. min. s.	LONG. (E) deg. min. s.	SYSTEM sensor recorder	START DATE	ORGANIZATION
KOB Alluvium	34 43 30.0	135 16 51.6	VSE11/12 CV901MVR Velocity	94/04-	CEORKA
FKE Reclaimed	34 42 58.7	135 17 36.9	VSE11/12 CR650 Acceleration	95/01/18	SHIMIZU
FKI Alluvium	34 43 05.2	135 16 53.1	VSE11/12 CR650 Acceleration	95/01/19	SHIMIZU
KMC Sand stone	34 43 47.0	135 17 10.8	VSE11/12 DRM2a Velocity	95/01/18	EGMDPRI
ASY Alluvium	34 43 27.4	135 18 30.6	VSE11/12 CR650 Acceleration	95/01/23	SHIMIZU
NOM Alluvium	34 43 17.8	135 16 20.7	VSE11/12 DRM2a Velocity	95/01/23	EGMDPRI

Table 2 Hypocenter parameters and trigger score of the Higashinada Ward array during the observation period from January 19 to February 18, 1995.

DATE M/D H:M:S	Lat. DEG. MIN. (N)	Long. DEG.MIN (E)	Dep. km	M_{JMA}	KMC	KOB	ASY	FKI	FKE	NOM
1/23 21:44:15.5	34 47.6	135 19.1	16.2	4.3	o	o	o	o	o	
1/25 23:15:57.2	34 47.4	135 18.8	16.7	4.7	o	o	o	o	o	
1/26 01:01:25.8	34 46.0	135 16.0	12.5	3.5	o	o	o	o	o	
1/29 00:27:12.7	34 44.2	135 17.0	8.6	2.9	o	o	o	o		o
1/31 08:24:18.3	34 44.4	135 17.3	10.8	3.2	o	o	o	o	o	o
2/ 2 16:19:28.0	34 41.7	135 09.0	17.9	4.2	o	o	o	o	o	o
2/ 3 20:36:55.3	34 43.8	135 16.0	11.5	3.4	o	o	o	o	o	o
2/18 21:37:33.9	34 26.7	134 48.4	12.6	4.9	o	o		o	o	o

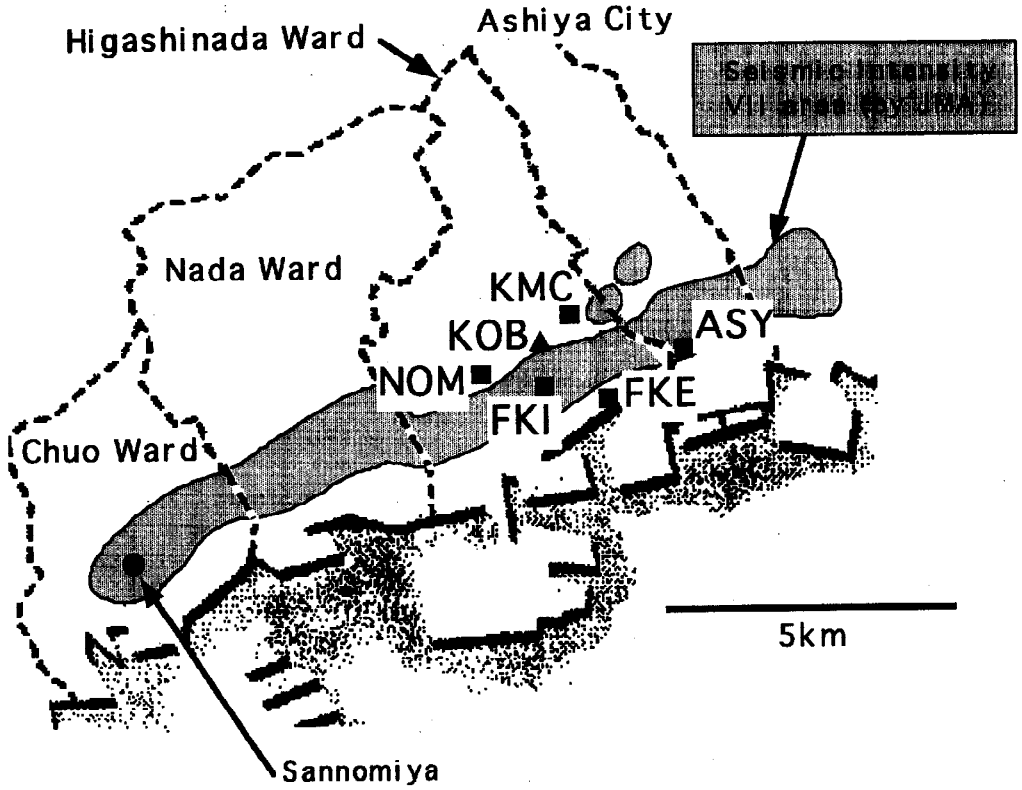

Fig. 1 Location of array observation stations in Higashinada Ward, Kobe City. Hatched area shows the seismic intensity of seven by JMA(1995).

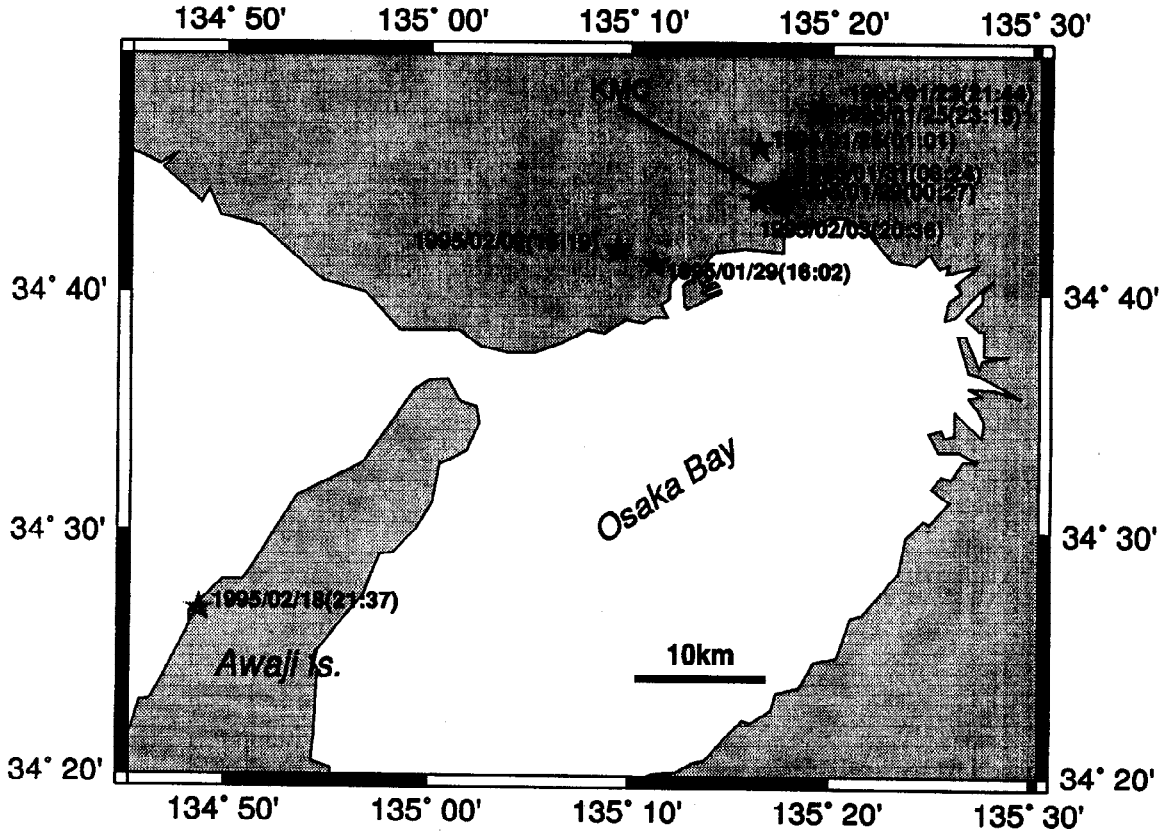

Fig. 2 Location map of the aftershocks used in this study together with the KMC station.

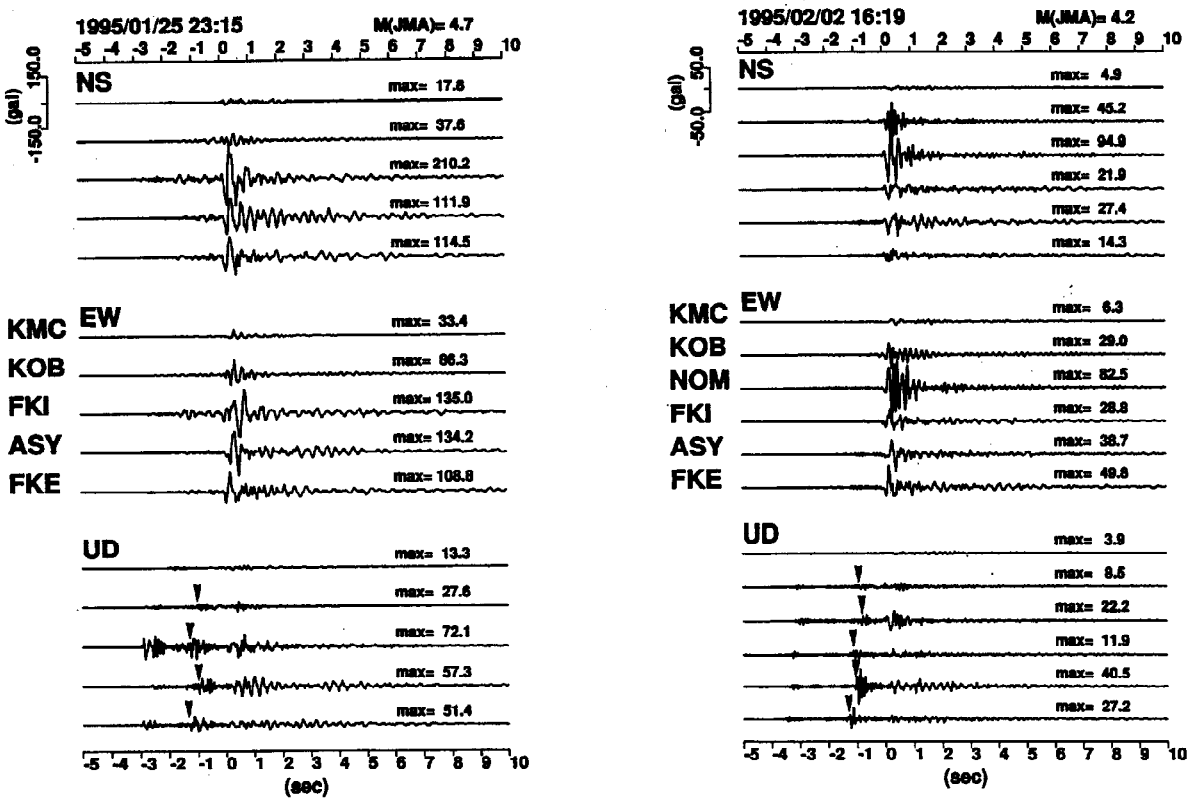

Fig. 3 Observed ground accelerations at array stations. Left: the event of 23:16, January 25, Right: the event of 16:19, February 2. From top to bottom: the NS, EW, and UD components of each station. Pasted-up seismic traces are arranged by S wave onset. Triangle ticks shown in the vertical motion traces are the SP converted waves of the interface between the bed rock and the sediment.

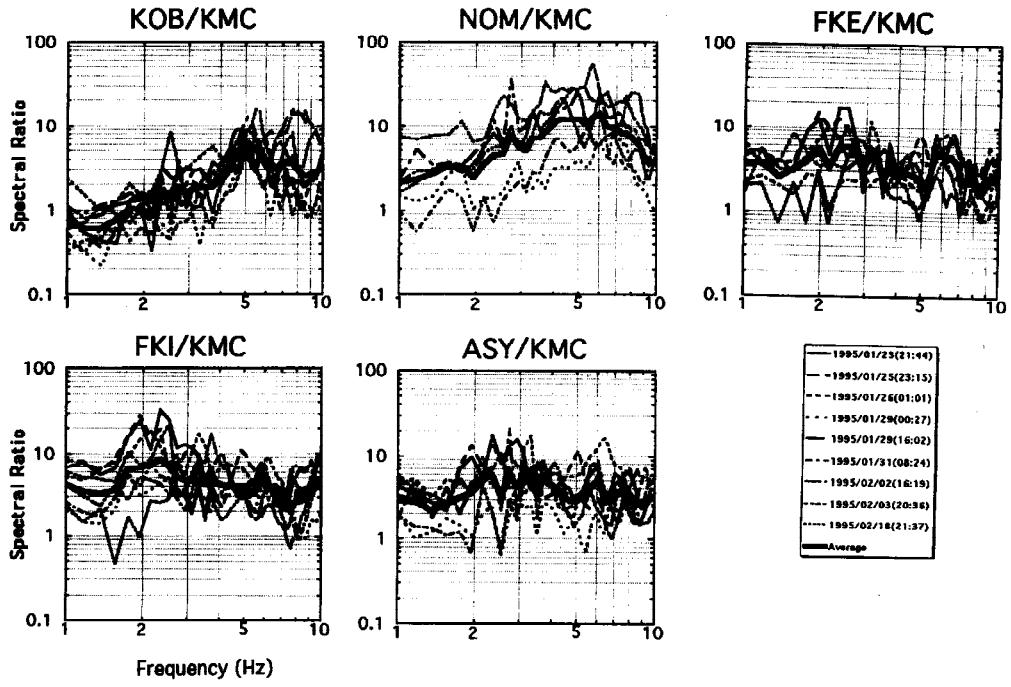

Fig. 4 S-wave amplitude spectral ratios of the vectorial summation of the two horizontal components of soil sites with the KMC station (rock site) as the reference point. Spectral ratios are calculated from the smoothed amplitude spectra of the 10% running mean.

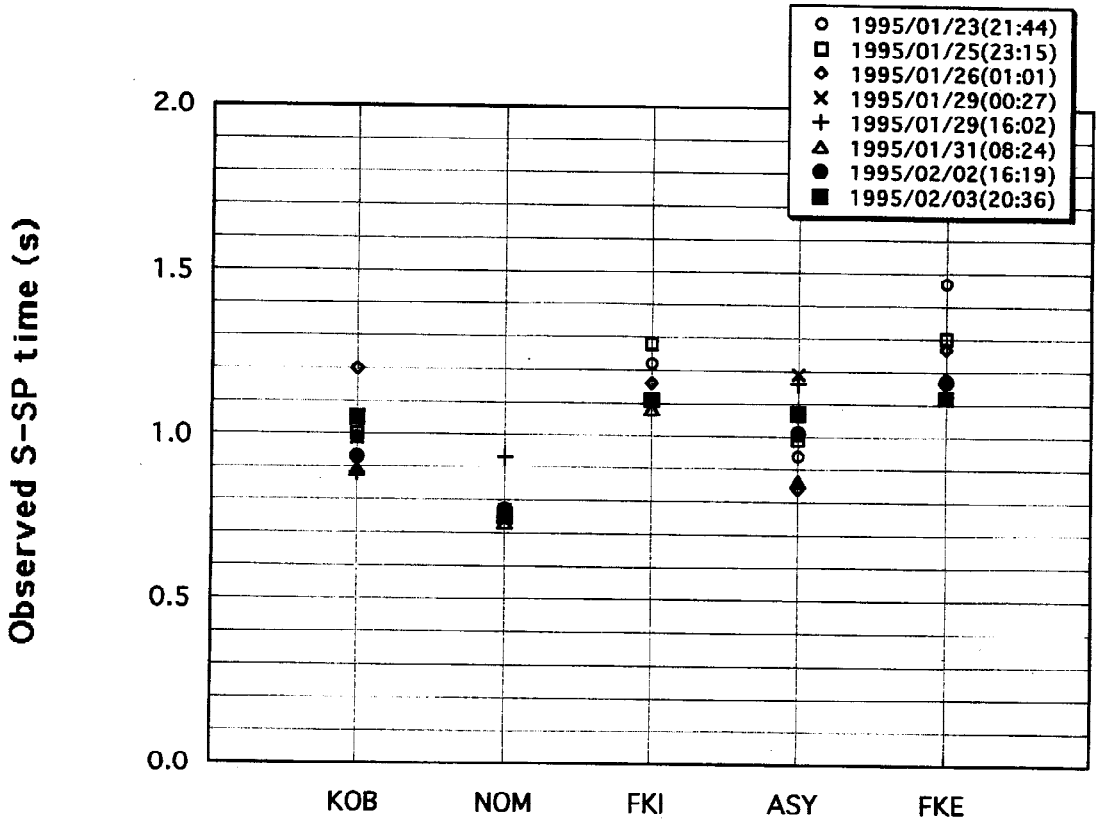

Fig. 5 Time differences between S and SP phases for each station.

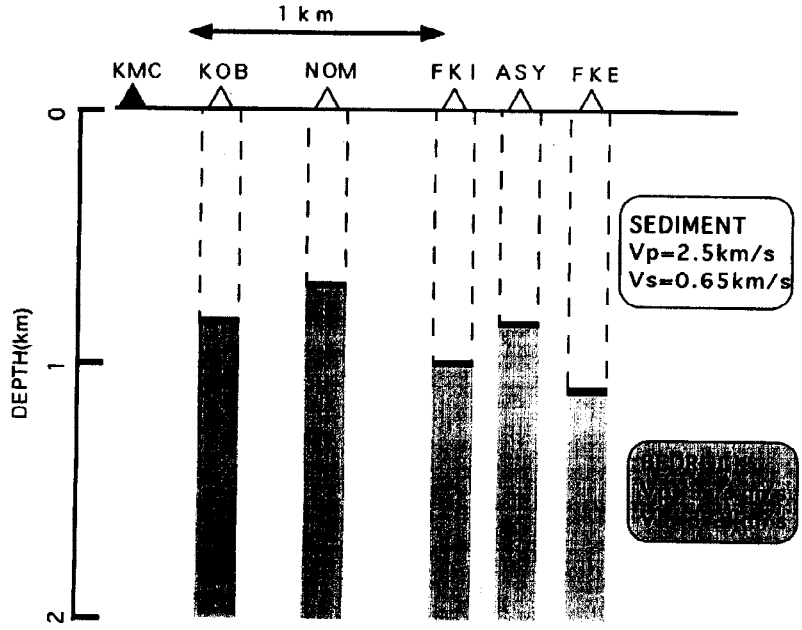

Fig. 6 Thickness of sediment under each observation station. Horizontal axis shows the distance from the edge of the basin.

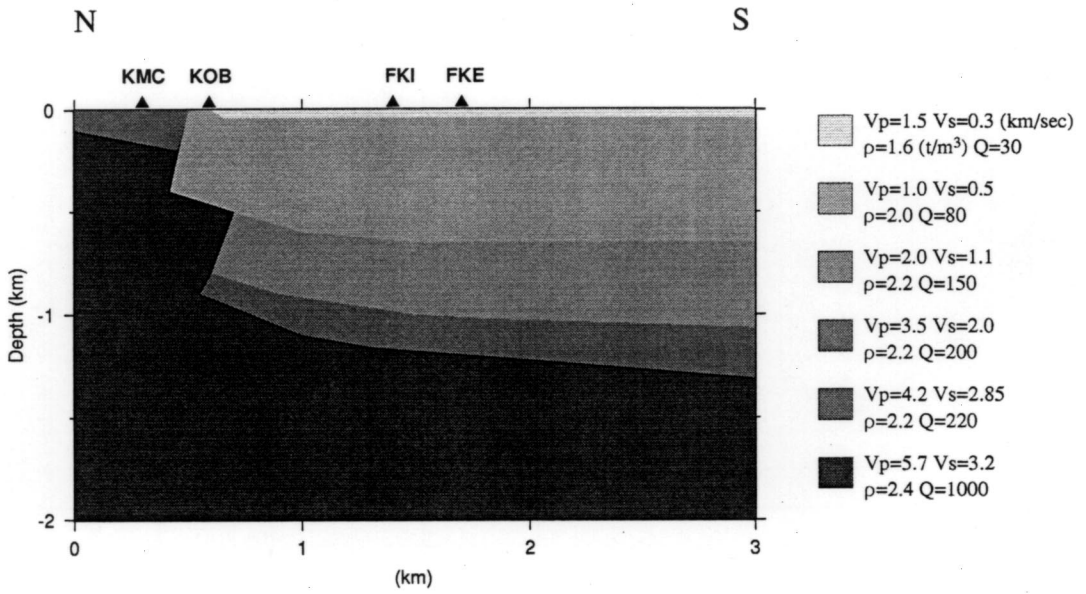

Fig. 7 Assumed basin structure beneath Higashinada array.

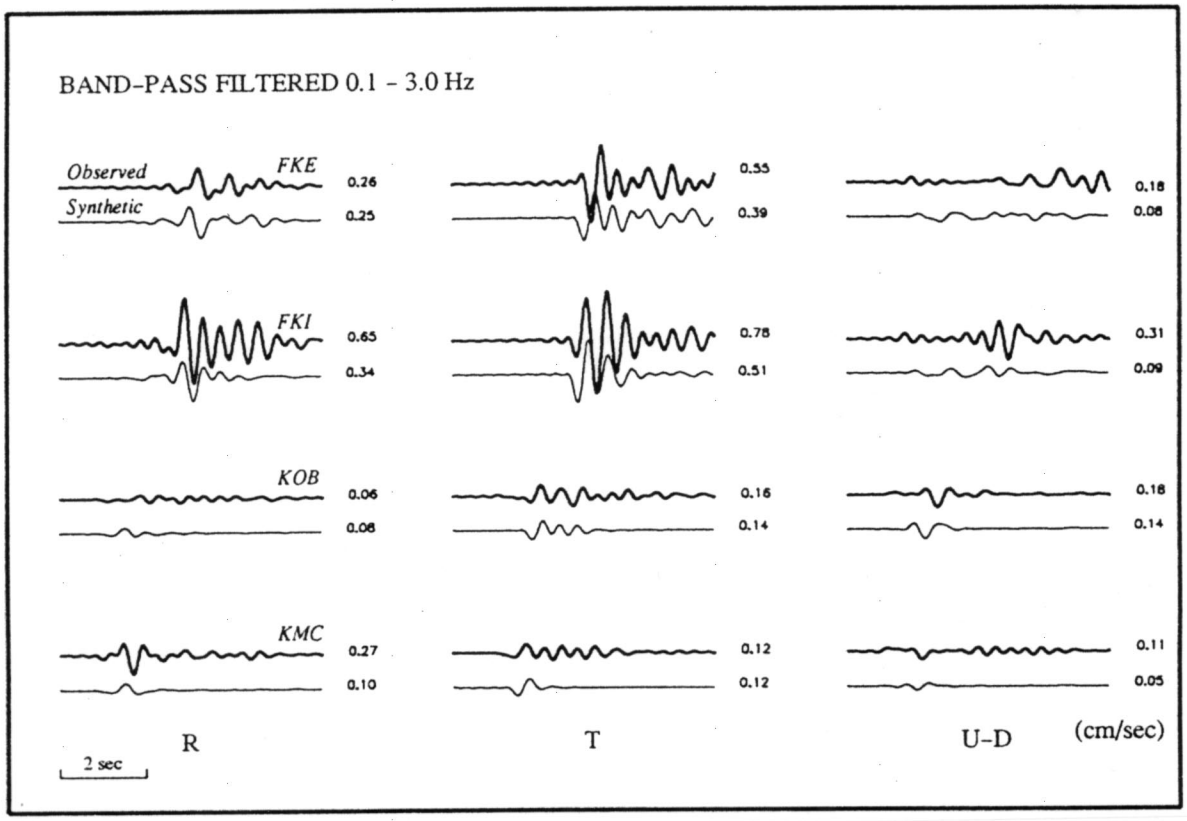

Fig. 8 Comparison of the synthetic with the observed velocity seismograms at the KMC, KOB, FKI, and FKE stations for the case of Jan. 25 event. The velocity model shown in Fig. 7 and a bell-shaped source time function with a pulse duration of 0.55s are used. Numbers attached to the seismograms are peak velocities in cm/s.